

Avatar Knowledge Distillation: Self-ensemble Teacher Paradigm with Uncertainty

Yuan Zhang*
zhangyuan@stu.pku.edu.cn
Peking University
Beijing, China

Tao Huang
huntocn@gmail.com
The University of Sydney
Sydney, Australia

Weihua Chen*
kugang.cwh@alibaba-inc.com
Alibaba Group
Beijing, China

Xiuyu Sun†
xiuyu.sxy@alibaba-inc.com
Alibaba Group
Beijing, China

Yichen Lu*
yicheng.lyc@alibaba-inc.com
Alibaba Group
Beijing, China

Jian Cao†
caojian@ss.pku.edu.cn
Peking University
Beijing, China

ABSTRACT

Knowledge distillation is an effective paradigm for boosting the performance of pocket-size model, especially when multiple teacher models are available, the student would break the upper limit again. However, it is not economical to train diverse teacher models for the disposable distillation. In this paper, we introduce a new concept dubbed *Avatars* for distillation, which are the inference ensemble models derived from the teacher. Concretely, (1) For each iteration of distillation training, various Avatars are generated by a perturbation transformation. We validate that Avatars own higher upper limit of working capacity and teaching ability, aiding the student model in learning diverse and receptive knowledge perspectives from the teacher model. (2) During the distillation, we propose an *uncertainty-aware* factor from the variance of statistical differences between the vanilla teacher and Avatars, to adjust Avatars' contribution on knowledge transfer adaptively. Avatar Knowledge Distillation (*AKD*) is fundamentally different from existing methods and refines with the innovative view of unequal training. Comprehensive experiments demonstrate the effectiveness of our Avatars mechanism, which polishes up the state-of-the-art distillation methods for dense prediction without more extra computational cost. The AKD brings at most **0.7 AP** gains on COCO 2017 for Object Detection and **1.83 mIoU** gains on Cityscapes for Semantic Segmentation, respectively.

CCS CONCEPTS

• **Computing methodologies** → **Object detection**; *Image segmentation*.

*Both authors contributed equally to this research.

†Correspondence to: Xiuyu Sun and Jian Cao.

Permission to make digital or hard copies of all or part of this work for personal or classroom use is granted without fee provided that copies are not made or distributed for profit or commercial advantage and that copies bear this notice and the full citation on the first page. Copyrights for components of this work owned by others than ACM must be honored. Abstracting with credit is permitted. To copy otherwise, or republish, to post on servers or to redistribute to lists, requires prior specific permission and/or a fee. Request permissions from permissions@acm.org.

MM '23, October 29 - November 02, 2023, Ottawa, Canada

© 2023 Association for Computing Machinery.

ACM ISBN 978-1-4503-8651-7/21/10...\$15.00

<https://doi.org/3474085.3475521>

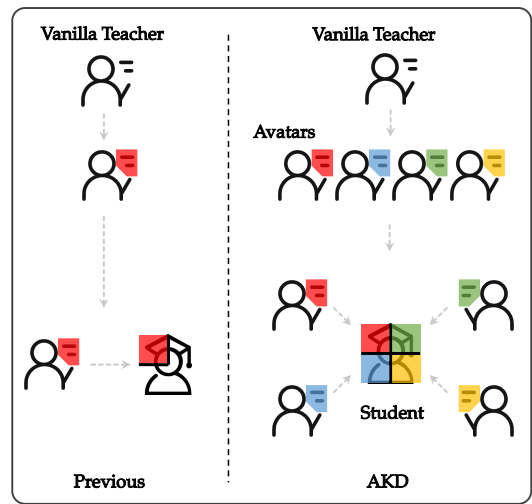


Figure 1: An illustration of Avatars distillation mechanism. Avatars ensemble not only owns stronger performance, but also more exquisite teaching skills than the vanilla teacher. Best view in color.

KEYWORDS

Model Compression, Knowledge Distillation, Avatars Mechanism, Object Detection

1 INTRODUCTION

Recent deep neural networks tend to grow deeper and wider for ultimate performance [17, 25, 44]. However, due to huge amounts of complicated parameters, such heavy models are clumsy and inefficient to deploy on edge devices, causing lower inference latency. To remedy the issue, knowledge distillation (KD) [18] has been proposed to inherit the dark knowledge from a heavy model (teacher) to a compact model (student) with similar structure, and make student generalize better than being trained alone.

Taking the advance of model ensemble, some recent methods [16, 29, 49] improve the distillation performance by employing multiple teachers to teach the student simultaneously. The basic motivation behind these methods is that, compared to single teacher, multiple

teachers can provide more various and informative supervisions to the student by generating diverse “views” of each given sample, and thus lead the student to generalize better [16, 49]. However, obtaining such diverse teachers requires to train multiple teachers, which is computationally-expensive, uneconomic, and ungreen.

In this paper, we aim to solve the above problem by proposing Avatar Knowledge Distillation (AKD), which only utilizes one teacher to generate such diverse “views” of samples in multiple teachers. Concretely, with the deterministic network parameters of a teacher, AKD leverages an efficient Bayesian perturbation in Bayesian Neural Networks (BNNs) [2, 22] to disturb the teacher features into multiple diverse features, which we call Avatars, to supervise the student. As alternates of multiple teachers, these Avatars can also provide multiple discriminate perspectives of data samples to enhance the student, as illustrated in Fig. 1.

Nevertheless, it is inevitable for Avatars to bring extra noises into distillation due to the perturbation, while these noises could mislead the student from learning beneficial knowledge. Therefore, how to control the stability of training process and reduce the impact of noise is a vital question deserved to explore. Recently, some methods propose adaptive weight schema to balance the influence of multiple teachers in distillation. For example, AMTML-KD [29] calculates the weights based on latent factors, while CA-MKD [51] affirms that the teacher’s predictions closer to the labels should be assigned to larger weights. However, such heuristic rules may not be ideal proxies to measure the contributions of each teacher, and therefore limit the distillation performance of multiple teachers. In this paper, considering that our Avatars are generated through Bayesian perturbation, we can naturally model the noise as an uncertainty from the generation, and leverage an uncertainty-aware factor to adjust the impact of Avatars on distillation. With the help of our uncertainty-aware weight, we could avoid the noise in Avatars damaging the knowledge transfer process.

As analyzed above, we propose an **Avatar Knowledge Distillation (AKD)**, involving multiple Avatars to ensemble distillation adaptively, as shown in Fig. 1. Various Avatars are only generated from intermediate features, so that AKD can be directly extended to existed methods on several vision tasks, including classification, object detection and semantic segmentation. Without bells and whistles, our method can further improve baseline algorithms and achieve state-of-the-art performances consistently on detection and semantic segmentation benchmarks. In a nutshell, the contributions of this paper are:

- (1) We design Avatar Knowledge Distillation (AKD), a self-ensemble teacher paradigm, to enrich the diversity for distillation, without the cost of training multiple teachers. The mechanism is simple but efficient, and orthogonal with other distillation methods.
- (2) An uncertainty-aware weight is modelled from the generation to measure the influence and stability of Avatars on distillation, which aids to weaken the negative effects from the noise in Avatars.
- (3) We verify the effectiveness of our method on object detection and semantic segmentation tasks via extensive experiments based on existed methods, achieving state-of-the-art performance.

2 RELATED WORK

2.1 Knowledge Distillation

As the seminal work by Hinton [18], knowledge distillation is introduced to boost performance of tiny models. A line of works [1, 30, 38, 50] has verified its potential. To extend its application to object detection, MIMIC [24] proposed to prevent divergence between RPN output of teacher and student via L_2 loss. To filter massive less informative supervision in background areas, Wang [40] transferred effective knowledge in sparse imitation regions. To handle imbalanced supervision from foreground and background pixels, Zhang [52] and Yang [45] encouraged student to learn from crucial pixels of foreground objects and the relationship between them. To separate informative feature in and out of bounding boxes, FRS [15] presented feature-richness score to focus on important features. To further investigate sophisticated dependence, MasKD [20] proposed receptive tokens to build pixel dependency masks for more effective distilling. Instead of spatial-wise, CWD [36] exploited more semantical information in each channel with category-specific masks. For the sake of fusing different kinds of information, GID [12] merged branches of feature/relation/response-based knowledge and developed an all-in-one framework. In most recent work MGD [46], distillation was combined with self-supervision task, it implicitly guided student via recovering teacher output with masked student features, introducing another generative way in distillation.

2.2 Multiple Teachers Distillation

Based on knowledge distillation with single teacher, multiple teachers could provide supervision from other more perspectives of data and lead to more impressive performance. Prior works conducted such teaching with an ensemble teacher [4] or with fixed weight average [43, 48] from multiple teachers. To better handle complex scenarios, with regard to each individual instance, each teacher responses differently and should be assigned with different weight adaptively. Following such idea, Liu [29] proposed to adaptively learning multi-level knowledge from teachers. Furthermore, CA-MKD [51] bases weight assignment strategy on confidence of teachers. AKDE [23] proposed that student should trust teachers that predict with lower entropy. In AE-KD [14], multiple teacher distillation is treated as a multi-objective optimization problem to encourage better optimization direction. Methods above are built on assumptions that better teacher supervision is related to higher confidence, lower entropy and similar gradients, etc. For better generalization, RL-KD [49] proposed to dynamically assign weights to multiple teachers with respect to different data with reinforcement learning.

However, as they named it, all of methods above are driven by multiple teachers, which is not economical and not practical in computational-limited scenarios. Expanding one teacher to its multiple avatars could provide a promising solution from another perspective. Because one teacher means more practical and multiple avatars bring more working capacity and teaching ability (as detailed in Sec. 3.1), which seems to be a free lunch in distillation.

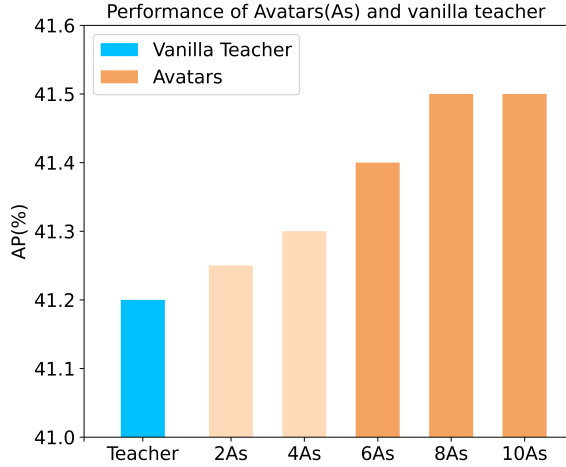


Figure 2: Experiment on the performance of ensemble Avatars based on *RetinaNet-X101* detector on COCO 2017.

2.3 Uncertainty Estimation in Computer Vision

Uncertainty describes the robustness in model inference. Kendall [21] formulated two types of uncertainty, epistemic uncertainty and aleatoric uncertainty from data and model respectively. Estimating such uncertainty denoises the training procedure and encourages model to learn from reliable operation with less ricks. And with this pronounced advantage, many works in face recognition [35, 54], person ReID [56], semantic segmentation [21, 57], object detection [41] and knowledge distillation [53], have justified uncertainty in computer vision. Uncertainty-based methods focus on the noise-resistant environments. In a standard pipeline, they suppose that uncertainty in data or prediction is strongly related to quality of supervision. And uncertainty could stem from noise in mislabelling, ill pseudo-labels, inconsistent output and so on. After quantifying the noise and turning it into uncertainty, methods scale the objective function and put more attention on reliable data with lower uncertainty.

Different from existing work, to our best knowledge, our work is the first exploration about uncertainty-aware teachers (Avatars) from the generation in distillation. In this paper, we quantify the uncertainty of each element in feature maps and dynamically assign weights to distillation term in the most refined way.

3 PROPOSED APPROACH

3.1 Multiple Avatars are Better than a Teacher

The Avatar A_i is generated by the perturbation P , whose feature maps $F^{(a_i)}$ stem from feature maps $F^{(t)}$ of teacher model T . The generation can be formulated as:

$$F^{(a_i)} = P(F^{(t)}), \quad (1)$$

where $F^{(a_i)} \in \mathbb{R}^{C \times H \times W}$ and $F^{(t)} \in \mathbb{R}^{C \times H \times W}$ denote the feature maps the student would be imitated (eg, the outputs of feature pyramid network [26] (FPN) in object detection tasks). Inspired

Table 1: Performance of the distilled student under the supervision of Avatars (equal weights ensemble) and vanilla teacher, respectively.

| Method | Supervisor | AP(%) |
|-----------|-----------------|-------------|
| CWD (KL) | Vanilla teacher | 40.8 |
| CWD (KL) | Avatars | 41.0 |
| MGD (MSE) | Vanilla teacher | 41.0 |
| MGD (MSE) | Avatars | 41.2 |

by [21], we use Bayesian Neural Network (BNN) [2, 22] as the perturbation P to produce our Avatars.

In our paper, we employ the single dropout operation instead of Multi-Layer Perception (MLP) to form the BNN, which is simple but effective, to avoid extra computational cost. Notably, other augmentation methods can also replace the dropout to function as the perturbation P , providing disturbance.

During Avatars distillation, one typical manner is to mimic the tensor pixel-wisely [5, 33]. The vanilla Avatars distillation can be completed via Avatars ensemble model A , when each avatar makes the equal contribution to the supervision:

$$\mathcal{L}_{\text{distill}}(A, S) = \frac{1}{k} \sum_i^k \frac{1}{HWC} \left\| F^{(a_i)} - \phi(F^{(s)}) \right\|_2^2, \quad (2)$$

where $F^{(s)}$ is the feature maps of the student model, k is the amount of Avatars and ϕ is a linear projection layer to adapt $F^{(s)}$ to the same resolution as $F^{(a_i)}$.

Next, we will demonstrate the reason that why multiple Avatars are better than a teacher on the following two aspects: Working capacity and Teaching ability.

Working capacity. We first validate the Avatars ensemble model owns a better working capacity on specific tasks. As shown in Fig. 2, we conduct the experiment on the performance of ensemble¹ Avatars and teacher on COCO dataset with RetinaNet-X101. When the number of Avatars exceeds one, their ensemble performance is constantly superior to teacher’s. Ensemble model always owns richer feature representation and stronger robustness compared with the single one, which is worthy of imitation.

Teaching ability. Besides, we further prove that the Avatars ensemble model affords more exhaustive guide for the student. Various data distribution in Avatars makes the student learn the diverse perspective of feature maps, and the unequal distillation ensures the student receive high-quality knowledge. As the experiments conducted in Tab. 1, we train the student *RetinaNet-R50* with Avatars (equal weights ensemble) and vanilla teacher *RetinaNet-X101* using $2 \times$ schedule, and adopts CWD (based on KL) and MGD (based on MSE) distillation on feature. Avatars constantly bring extra gain (0.2 AP) on distillation, proving that choosing multiple Avatars is a better schema.

The generation of Avatars is presented in Fig. 3. The perturbation applies on the feature maps from the teacher, and produce k Avatars in each iteration, which boost the performance of student.

¹Weighted Box Fusion (WBF) [37] is used to ensemble Avatars’ outputs

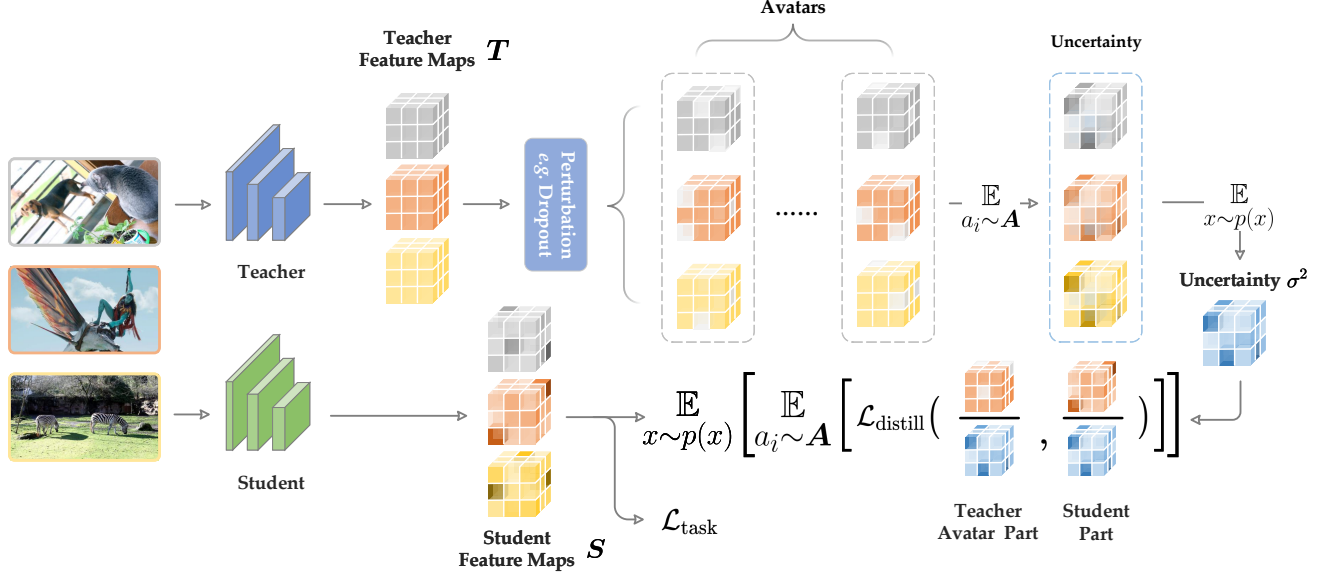


Figure 3: Overview of our AKD framework. Teacher feature maps separated into N avatars, containing diverse perspective knowledge. To measure the quality of each randomly perturbed avatars, uncertainty is introduced and calculated among all avatars of training data. Combining the merged uncertainty to scale affects adaptively on dimensions (e.g. channels, spatial grids), distillation process is conducted between student and teacher avatars.

3.2 The Uncertainty-Aware Weight

However, when the Avatars are produced, the perturbation not only brings diversity into the Avatars, but also involves the noise that may drift the Avatar from the original teacher and even lead to a lower performance. The noise and the diversity is a tricky balance for the Avatars. Hence, we have to find a way to watch the generation, and reduce Avatars' effects on distillation when the noise impact becomes severe.

During the generation, there exists disagreement between a specific Avatar output $F^{(a_i)}$ and the teacher output $F^{(t)}$, i.e., $F^{(a_i)} = F^{(t)} + \mathbf{n}$, caused by the perturbation. Assuming that the noise \mathbf{n} follows a normal distribution $\mathcal{N}(0, \sigma_i)$, the posterior of each sample can be formulated as:

$$p(F^{(a_i)}|x) = \frac{1}{\sqrt{2\pi}\sigma_{ix}^2} \exp\left(-\frac{(F^{(a_i)} - F^{(t)})^2}{2\sigma_{ix}^2}\right) \quad (3)$$

where σ_{ix} is the variance for input data x on Avatar i . In [21], σ_{ix} is treated as epistemic uncertainty, which is employed for measuring the potential variance of the model. The Avatar output $F^{(a_i)}$, the teacher output $F^{(t)}$ and the variance σ_{ix} are all given in form of tensor, i.e., $\{F^{(a_i)}, F^{(t)}, \sigma_{ix}\} \in \mathbb{R}^{C \times H \times W}$. After traversing over all possible samples, posterior turns into the equation below:

$$p(F^{(a_i)}|x) = \mathbb{E}_{x \sim p(x)} \left[\frac{1}{\sqrt{2\pi}\sigma_{ix}^2} \exp\left(-\frac{(F^{(a_i)} - F^{(t)})^2}{2\sigma_{ix}^2}\right) \right], \quad (4)$$

$p(F^{(a_i)}|x)$ is the posterior for Avatar i . To minimize the negative log likelihood of posterior, the objective is achieved across all Avatars:

$$\begin{aligned} \mathcal{L}_{\text{uncertainty}}(x) &= -\log p(A|x) \\ &= \mathbb{E}_{x \sim p(x)} \left[\mathbb{E}_{a_i \sim A} \left[\frac{1}{2} \log 2\pi\sigma_{ix}^2 + \frac{(F^{(a_i)} - F^{(t)})^2}{2\sigma_{ix}^2} \right] \right] \\ &\propto \mathbb{E}_{x \sim p(x)} \left[\mathbb{E}_{a_i \sim A} \left[\underbrace{\log \sigma_{ix}^2 + \frac{(F^{(a_i)} - F^{(t)})^2}{\sigma_{ix}^2}}_{\text{local}} \right] \right]. \end{aligned} \quad (5)$$

For the local uncertainty term, it will reach analytical minimum, when we let $\sigma_{ix}^2 = (F^{(a_i)} - F^{(t)})^2$.

Considering the whole generation, the optimal uncertainty σ will converge to $\sigma^2 = \mathbb{E}_{x \sim p(x)} \left[\mathbb{E}_{a_i \sim A} \left[(F^{(a_i)} - F^{(t)})^2 \right] \right]$ across all Avatars and all data. Here with the dropout operation as an example, i.e., $F^{(a_i)} = \text{dropout}(F^{(t)}, 1 - m_i)$, where m_i is the corresponding dropout ratio, the uncertainty σ of the whole generation could be further simplified:

$$\begin{aligned} \sigma^2 &= \mathbb{E}_{x \sim p(x)} \left[\mathbb{E}_{a_i \sim A} \left[(F^{(a_i)} - F^{(t)})^2 \right] \right] \\ &= \mathbb{E}_{x \sim p(x)} \left[m_i^2 \left[F^{(t)} \right]^2 \right] \\ &\stackrel{\mu_{x \sim p(x)}[F^{(t)}]=0}{\propto} m_i^2 \times \text{var}_{x \sim p(x)} \left[F^{(t)} \right] \\ &\propto \text{var}_{x \sim p(x)} \left[F^{(t)} \right], \end{aligned} \quad (6)$$

From Eq. 6, it can be found that the uncertainty (the noise brought by the perturbation) is directly proportional to the dropout ratio term m_i^2 and the statistical variance of the teacher across all data $\text{var}_{x \sim p(x)} [F^{(t)}]$, under the condition of $\mu_{x \sim p(x)} [F^{(t)}] = 0$. It is noteworthy that the condition $\mu_{x \sim p(x)} [F^{(t)}] = 0$ could be easily achieved by estimating and subtracting mean of global features. In this paper, we involve a Batch Normalization (BN) Layer after the teacher feature maps T before the perturbation P (i.e., dropout) to achieve $\mu_{x \sim p(x)} [F^{(t)}] = 0$. And the dropout ratio term m_i^2 can be set to a fixed value and controlled manually. So that the uncertainty is proportional to the statistical variance of the teacher across all data $\text{var}_{x \sim p(x)} [F^{(t)}]$. Finally, the uncertainty is obtained by Eq. 6 with the form of variance of each position in tensor $\mathbb{R}^{C \times H \times W}$ and could be further merged (e.g. in channel-wise or spatial-wise) to get a more stable form. Detailed discussion is reported in Sec. 5.2.

To plug the uncertainty-aware weight, the eventual distillation objective \mathcal{L}_{AKD} is formulated as:

$$\mathcal{L}_{\text{AKD}}(S, A) = \frac{1}{k} \sum_i \frac{1}{\text{HWC}} \left\| \frac{F_{c,h,w}^{(a_i)}}{\sigma_{c,h,w}} - \frac{\phi(F^{(s)})_{c,h,w}}{\sigma_{c,h,w}} \right\|_2^2 \quad (7)$$

3.3 Discussion

Uncertainty of Whole Feature Maps. In previous works on uncertainty [21, 53], typically, a scalar is estimated to measure the noise in each sample and put more weight to cleaner data. In our approach, uncertainty is a tensor to reflect the variance of whole feature maps. Due to the statistics from global feature distribution, attention is put more precisely on different positions and induces better performance of student networks.

Dynamic and General Temperature. In vanilla distillation [18], temperature is proposed to produce a softer distribution over classes. In normal cases, distribution over classes could be described in single dimension, and a fixed temperature is enough to balance between details with lower probability and majority with higher probability. However, when it comes to distilling towards features in detection, more dimensions make it more troublesome to handle the variance in different dimensions. Over-softened features lose attention on foreground and under-softened features lead to ignorance of subtle changes. To relieve such flaw, our uncertainty could be viewed as dynamic temperature towards feature (or feature block) in different position. Besides, the concept of temperature is more general with uncertainty. It will not be limited in form of KL divergence. In terms of gradients, the general form is written as:

$$\frac{\partial \mathcal{L}}{\partial F_{c,h,w}^{(s)}} = \frac{\partial \mathcal{L}_{\text{distill}}(F_{c,w,h}^{(t)}/\sigma_{c,w,h}, F_{c,w,h}^{(s)}/\sigma_{c,w,h})}{\sigma_{c,h,w} \partial F_{c,h,w}^{(s)}}. \quad (8)$$

Here, we take two types of widely-used loss function, i.e., MSE and KL, as examples:

$$\frac{\partial \text{MSE}(\frac{F_{c,h,w}^{(t)}}{\sigma_{c,h,w}}, \frac{F_{c,h,w}^{(s)}}{\sigma_{c,h,w}})}{\partial F_{c,h,w}^{(s)}} = \frac{2(F_{c,h,w}^{(s)} - F_{c,h,w}^{(t)})}{\sigma_{c,h,w}^2}, \quad (9)$$

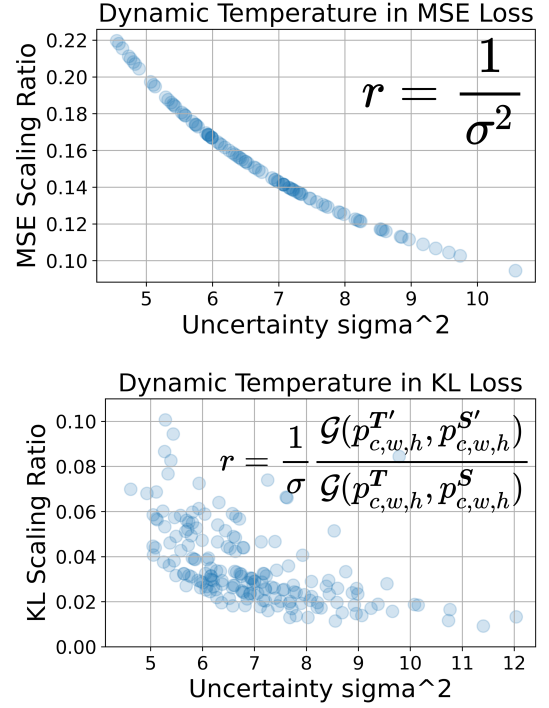


Figure 4: Impact of uncertainty on gradients. We plot scatter: ratio of gradient v.s. uncertainty, where ratio of gradient could be described as $r = \text{grad}_{w/\sigma} / \text{grad}_{w/o \sigma}$. We take MSE loss (Left) and KL loss (Right) as examples and their ratio formulas are pinned on top right corners. Note that $\mathcal{G}(\cdot)$ in KL plot is formulated in Eq. 10.

$$\frac{\partial \text{KL}(p_{c,w,h}^T, p_{c,w,h}^S)}{\partial S_{c,h,w}} = \frac{\mathcal{G}(p_{c,w,h}^T, p_{c,w,h}^S)}{\sigma_{c,h,w}}, \quad (10)$$

$$\mathcal{G}(p_{c,w,h}^T, p_{c,w,h}^S) = p_{c,w,h}^S \sum_{i,j,k} p_{i,j,k}^T - p_{c,h,w}^T$$

where $p_{c,h,w}^{T/S} = \text{softmax}(F_{c,h,w}^{(t)/(s)} / \sigma_{c,h,w})$. In formulas, uncertainty plays the role of temperature and gradients are all scaled adaptively as illustrated in Fig. 4.

4 EXPERIMENTS

The AKD is a novel distillation mechanism that can easily be applied to different models for various tasks. In this section, to verify the compatibility of our approach on vision tasks (including classification, object detection and semantic segmentation), we plug AKD into three advanced feature-based distillation schema (including CWD [36] from ICCV 2021, MGD [46] from ECCV 2022 and MasKD [20] from ICLR 2023) based on MMRazor [9].

4.1 Classification

4.1.1 Datasets. We validate our Avatars distillation efficacy on ImageNet-1K [13] for classification, which contains 1000 object categories. We use the 1.2 million images for training and evaluate the student networks with accuracy (Acc) on 50k images.

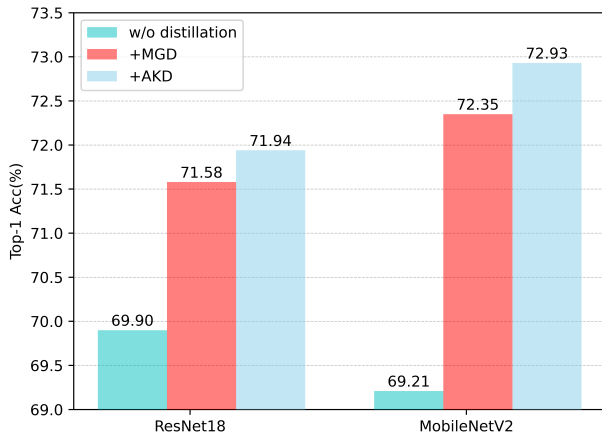


Figure 5: Performance of various KD strategies for classification (Top-1).

4.1.2 Network architectures. We follow MGD [46], including homogeneous and heterogeneous distillation. Conduct comprehensive experiments on different detection frameworks, the one distillation setting is from ResNet-R34 [17] to ResNet-R18, the other is from ResNet-R50 to MobileNetV2-R18 [34].

4.1.3 Implementation Details. For the classification task, the feature maps of Avatars source from last feature map in the backbone of teacher. All the models are trained with the official strategies of 100 epochs schedule in MMClassification [10] with SGD optimizer based on Pytorch, where the momentum is 0.9 and the weight decay is $1e-4$. We initialize the learning rate to 0.1 and decay it for every 30 epochs. This setting is based on 8 V100 GPUs.

4.1.4 Experimental results. We transfer feature-based knowledge from backbone instead of logits-based knowledge. As shown in Fig. 5, compared with only by MGD distillation, the student ResNet-R18 and MobileNet-R18 gain 0.36 and 0.58 Top-1 accuracy improvement with our method, respectively. Various Avatars with adaptive weights further provide more robust and receptive feature maps information for the student.

4.2 Object detection

4.2.1 Datasets. We validate our Avatars distillation efficacy on MS COCO detection dataset [28] for object detection, which contains 80 object classes. We evaluate the student networks with average precision (AP) on val2017 set.

4.2.2 Network architectures. we conduct comprehensive experiments on different detection frameworks, including two-stage models [32], anchor-based one-stage models [27], and anchor-free one-stage models [39, 47] to show our method effectiveness.

4.2.3 Implementation Details. For the detection task, the feature maps of Avatars source from feature maps in the neck of teacher. We adopt ImageNet pre-trained backbones during training and inheriting strategy following previous KD works [46]. All the models are trained with the official strategies (SGD, weight decay

Table 2: Object detection performance with Avatars in baseline settings on COCO val set. CM RCNN: Cascade Mask RCNN.

| Method | AP | AP ₅₀ | AP ₇₅ | AP _S | AP _M | AP _L |
|---------------------|-------------|------------------|------------------|-----------------|-----------------|-----------------|
| T: Faster RCNN-R101 | 39.8 | 60.1 | 43.3 | 22.5 | 43.6 | 52.8 |
| S: Faster RCNN-R50 | 38.4 | 59.0 | 42.0 | 21.5 | 42.1 | 50.3 |
| CWD [36] | 40.5 | 60.8 | 44.0 | 23.3 | 44.6 | 53.4 |
| + AKD | 40.8 | 61.0 | 44.7 | 23.4 | 44.6 | 53.9 |
| MasKD [20] | 40.6 | 60.7 | 44.2 | 23.0 | 44.0 | 53.9 |
| + AKD | 40.9 | 60.9 | 44.7 | 23.3 | 44.5 | 54.1 |
| T: RetinaNet-R101 | 38.9 | 58.0 | 41.5 | 21.0 | 42.8 | 52.4 |
| S: RetinaNet-R50 | 37.4 | 56.7 | 39.6 | 20.0 | 40.7 | 49.7 |
| CWD [36] | 39.8 | 59.0 | 42.6 | 21.7 | 43.5 | 53.4 |
| + AKD | 40.2 | 59.1 | 42.8 | 22.2 | 44.0 | 54.7 |
| MasKD [20] | 39.9 | 59.0 | 42.7 | 21.4 | 43.6 | 53.8 |
| + AKD | 40.3 | 59.4 | 43.0 | 21.8 | 44.1 | 54.2 |
| T: FCOS-R101 | 40.8 | 60.0 | 44.0 | 24.2 | 44.3 | 52.4 |
| S: FCOS-R50 | 38.5 | 57.7 | 41.0 | 21.9 | 42.8 | 48.6 |
| CWD [36] | 42.4 | 60.9 | 45.9 | 25.8 | 46.8 | 53.6 |
| + AKD | 42.9 | 61.3 | 46.5 | 26.6 | 46.8 | 54.8 |
| MasKD [20] | 42.2 | 60.9 | 45.6 | 26.2 | 46.4 | 53.6 |
| + AKD | 42.5 | 61.2 | 46.0 | 26.5 | 46.8 | 54.0 |

of $1e-4$) of 2X schedule in MMDetection [6]. We run all the models on 8 V100 GPUs.

4.2.4 Experimental Results on Baseline Avatars. For thoughtful experiments, we first follow MasKD, and adopt multiple detection frameworks for our baseline settings, including two-stage detector Faster-RCNN, one-stage detector RetinaNet, and anchor-free detector FCOS. We take ResNet-101 (R101) backbone as the teacher network, with ResNet-50 (R50) as the student.

As shown in Tab. 2, our method indeed can further boost the performance of the two baseline algorithms. From the results that we report, Avatar mechanism steadily brings an increase of **0.3+ AP** gain (at most **0.5**) for CWD and MasKD, while under the same training setting. The result indicates that our method fits for different detection frameworks. Besides, the uncertainty-aware weight in AKD is suitable for both KL (average 0.40 AP gain on CWD) and MSE (average 0.33 AP gain on MasKD) loss function.

4.2.5 Experimental Results on Stronger Avatars. Following CWD and MGD, we conduct experiments on stronger teacher detectors, including two-stage detector Cascade Mask RCNN [3], one-stage detector RetinaNet, and anchor-free detector RepPoints, with stronger backbone ResNeXt101 (X101) [44].

The results in Tab. 3 demonstrate that, even if compared with stronger vanilla teachers, our method still can further improve the performance of distillation. For example, AKD brings **0.7 AP** gain on retinaNet for CWD and **0.5 AP** gain on RepPoints for

MGD, which are practical and huge improvements to detection distillation. Besides, we find that AKD affords more support to detecting large size objects (AP_L), as larger objects would involve more data disturbance when generating Avatars. From another perspective, distillation of one-stage detectors is more sensitive to Avatar mechanism, where it brings about 0.4 to 0.7 AP gain, and we assume that it is uncertainty-aware weight that filters more semantic information, filling the gap with the two-stage detectors.

Table 3: Object detection performance with stronger Avatars on COCO val set. CM RCNN: Cascade Mask RCNN.

| Method | AP | AP ₅₀ | AP ₇₅ | AP _S | AP _M | AP _L |
|--------------------|-------------|------------------|------------------|-----------------|-----------------|-----------------|
| T: CM RCNN-X101 | 45.6 | 64.1 | 49.7 | 26.2 | 49.6 | 60.0 |
| S: Faster RCNN-R50 | 38.4 | 59.0 | 42.0 | 21.5 | 42.1 | 50.3 |
| CWD [36] | 41.7 | 62.0 | 45.5 | 23.3 | 45.5 | 55.5 |
| + AKD | 42.0 | 62.3 | 45.7 | 23.6 | 45.9 | 55.7 |
| MGD [46] | 42.1 | 62.0 | 45.9 | 23.7 | 46.4 | 56.1 |
| + AKD | 42.4 | 62.4 | 46.1 | 23.7 | 46.8 | 56.5 |
| T: RetinaNet-X101 | 41.2 | 62.1 | 45.1 | 24.0 | 45.5 | 53.5 |
| S: RetinaNet-R50 | 37.4 | 56.7 | 39.6 | 20.0 | 40.7 | 49.7 |
| CWD [36] | 40.8 | 60.4 | 43.4 | 22.7 | 44.5 | 55.3 |
| + AKD | 41.5 | 60.8 | 44.4 | 22.9 | 45.9 | 55.5 |
| MGD [46] | 41.0 | 60.3 | 43.8 | 23.4 | 45.3 | 55.7 |
| + AKD | 41.4 | 60.7 | 44.1 | 23.5 | 45.9 | 55.9 |
| T: RepPoints-X101 | 44.2 | 65.5 | 47.8 | 26.2 | 48.4 | 58.5 |
| S: RepPoints-R50 | 38.6 | 59.6 | 41.6 | 22.5 | 42.2 | 50.4 |
| CWD [36] | 42.0 | 63.0 | 45.3 | 24.1 | 46.1 | 55.0 |
| + AKD | 42.3 | 63.1 | 45.4 | 24.1 | 46.4 | 55.9 |
| MGD [46] | 42.3 | 62.8 | 45.6 | 24.4 | 46.2 | 55.9 |
| + AKD | 42.8 | 63.5 | 46.1 | 24.5 | 47.0 | 57.3 |

4.3 Semantic segmentation

4.3.1 Datasets. We conduct experiments on Cityscapes dataset [11] to validate Avatars’ teaching ability, which contains 5000 high-quality images (2975, 500, and 1525 images for the training, validation, and testing). We evaluate all the student networks with mean Intersection-over-Union (mIoU).

4.3.2 Network architectures. For all segmentation experiments, we take PSPNet-R101 [55] as the teacher network. While for the students, we use various frameworks (DeepLabV3 [7] and PSPNet) with ResNet-18 (R18) to valid the effectiveness of our method.

4.3.3 Implementation Details. For the semantic segmentation task, the feature maps of Avatars source from last feature map in the backbone of teacher. We conduct experiments following CWD and MasKD. All the models are trained with the official strategies of 40K iterations schedule with 512×1024 input size in MMSegmentation [8], where the optimizer is SGD and the weight decay is $5e-4$. A

Table 4: Semantic segmentation performance with Avatars on Cityscapes val set. FLOPs is measured based on an input size of 512×1024 .

| Method | Params(M) | FLOPs(G) | mIoU (%) |
|------------------|-----------|----------|--------------|
| T: PSPNet-R101 | 70.43 | 574.9 | 78.34 |
| S: PSPNet-R18 | | | 69.85 |
| CWD [36] | | | 72.74 |
| + AKD | 12.9 | 507.4 | 74.57 |
| MGD [46] | | | 74.46 |
| + AKD | | | 76.00 |
| S: DeepLabV3-R18 | | | 73.20 |
| CWD [36] | | | 74.34 |
| + AKD | 13.6 | 572.0 | 75.02 |
| MGD [46] | | | 76.02 |
| + AKD | | | 76.42 |

polynomial annealing learning rate scheduler is adopted with an initial value of 0.02. We run all the models on 8 V100 GPUs.

4.3.4 Experimental results. As shown in Tab. 4, AKD further improves the performance of state-of-the-art distillation methods for semantic segmentation. Both the homogeneous and heterogeneous Avatar distillation bring the students significant improvements, e.g., the ResNet-18 based PSPNet gets at most **6.15 mIoU** improvement and that based DeepLabV3 gets **3.22 mIoU**. Notably, although the increase of DeepLabV3-R18 is lower than that of PSPNet, AKD still can bring at least 0.42 mIoU gain even if MGD already distills for DeepLabV3 perfectly.

5 ANALYSIS

Table 5: Ablation of components in AKD. We train the student RetinaNet-R50 with teacher RetinaNet-X101 using $2 \times$ schedule, and adopts CWD (based on KL) and MGD (based on MSE) distillation on feature.

| Method | Avatars Uncertainty | | AP(%) |
|-----------|---------------------|---|-----------------|
| | ✗ | ✗ | 40.8 (baseline) |
| CWD (KL) | ✓ | ✗ | 41.0 (+0.2 AP) |
| | ✓ | ✓ | 41.5 (+0.7 AP) |
| | ✗ | ✗ | 41.0 (baseline) |
| MGD (MSE) | ✓ | ✗ | 41.2 (+0.2 AP) |
| | ✓ | ✓ | 41.4 (+0.4 AP) |

5.1 Why Uncertainty for Evaluation Quality

To validate our uncertainty-aware weight effectiveness, we choose several common unequal training modules (SE [19], SAM [58], and

Table 6: The comparison of unequal training module on COCO (AP) with CWD. Teacher: RetinaNet-X101. Student: RetinaNet-R50.

| Teacher | Student | SE module [19] | SAM module [58] | CBAM module [42] | Uncertainty Ours |
|---------|---------|-------------------|--------------------|---------------------|---------------------|
| 41.2 | 37.4 | 41.1 | 40.9 | 41.1 | 41.5 |

CBAM [42]) to watch Avatars distillation. The results are reported on Tab. 6. We find that discriminating Avatars from channel or spatial or both of them dimension indeed works (0.1 AP), but the improvement they brought is far lower than uncertainty-aware weight brought. Our uncertainty-aware weight models the noise from Avatars generation, and force “mutant” Avatars to lower their effects to the student, instead of simple information redistribution. What’s more, as shown in Tab. 5, the uncertainty-aware weight improves our Avatar mechanism by +0.2 AP, it well restrains the negative Avatars during the random generation.

5.2 How to Merge Uncertainty

Table 7: Results of uncertainty mergence in different dimensions. We train the student *RetinaNet-R50* with teacher *RetinaNet-X101* using $2\times$ schedule and adopts CWD as distillation term. Chan.: Channel-wise, Spat.: Spatial-wise and Bat.: Batch-wise.

| Chan. | Spat. | σ^2 Across | σ^2 shape | AP(%) |
|-------|-------|----------------------|-----------------------|-----------------|
| ✓ | ✓ | Bat. + Chan. + Spat. | $1 \times 1 \times 1$ | 40.8 (baseline) |
| ✗ | ✗ | Bat. | $C \times H \times W$ | 41.0 (+0.2 AP) |
| ✗ | ✓ | Bat. + Spat. | $C \times 1 \times 1$ | 41.5 (+0.7 AP) |
| ✓ | ✗ | Bat. + Chan. | $1 \times H \times W$ | 41.2 (+0.4 AP) |

In our previous statement in Sec. 3.2, mergence of uncertainty in certain dimensions provides a more stable form for distillation. We now discuss how to merge uncertainty simply from channel-wise and spatial-wise perspectives with Tab. 7. Merging uncertainty in all dimensions gives a fixed scalar, which is equivalent to fixed temperature in CWD and serves as baseline. Comparing with baseline, using uncertainty across batch and spatial yields the best performance with 41.5 AP. And other two solutions (uncertainty across batch and across batch + channel + spatial) report 0.2 and 0.4 AP improvement over baseline. However, these two solutions all suffer from σ^2 shape mismatching problems when networks are trained with multi-scale images. To address it, interpolation has to be leveraged. Consequently it will lose some information in σ^2 tensor and hurt the performance. But the consistent improvements over baseline still reveal the effectiveness of the proposed uncertainty-aware weight.

5.3 Visualization

We visualize the heatmaps generated by AblationCAM [31] in Fig. 6 to further investigate effect of AKD. In the image, a player is swinging his tennis racket. RetinaNet-R50 detects the player and his

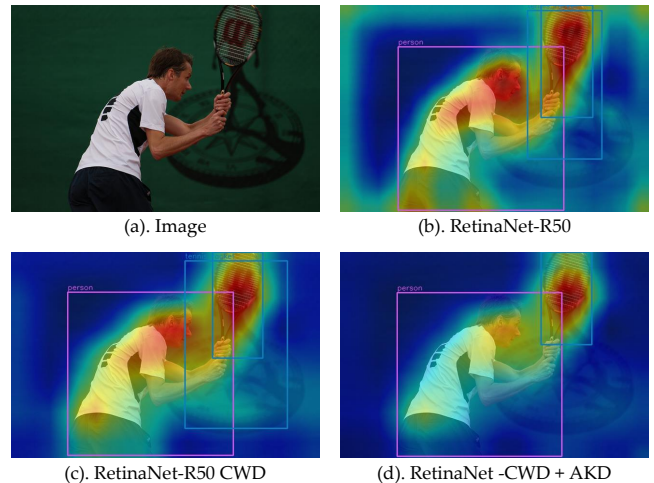


Figure 6: Comparison of feature maps with baselines. We compare our method with RetinaNet-R50 (w/o distillation), RetinaNet-R50 distilled by RetinaNet-X101 with CWD. The image is randomly selected from val set of COCO dataset and the heatmaps are generated with AblationCAM.

tennis racket successfully. However, the model confusingly spares attention to four corners and generates redundant bounding box of racket. After distillation, RetinaNet-R50 CWD tackles attention problem. It focuses more on the foreground, but still detects two racket by mistake. On this basis, our method yields no repeat bounding box. When comparing heat maps of RetinaNet-R50 CWD and RetinaNet-CWD + AKD, the latter spare less attention on the player and seems to perform worse than the former. However, in fact, our method further gathers attention on the player and racket rather than the background, especially the misleading logo on the ground. And as the result, AKD yields more clear contrast between background and foreground in heat map and it is important to produce the accurate bounding boxes in latter process.

6 CONCLUSIONS

In this paper, we propose our novel *AKD* framework to achieve impressive distillation performance when only one teacher model is available. In AKD, we put forward a concept called *Avatars*. Each Avatar stems from the same teacher and provides unique description of teacher output. Combining all Avatars of one teacher, various perspectives of knowledge are accessible, like multiple teachers. Moreover, *uncertainty-aware* weight is introduced. It takes statistical differences between the teacher and Avatars into consideration and balances importance Avatars in distillation adaptively. To investigate the effect of AKD, extensive experiments are conducted on classification, object detection and semantic segmentation. And encouraging SOTA results are observed on COCO and Cityscapes datasets when compared with other distillation algorithms, validating our motivation and approach.

REFERENCES

- [1] Sungsoo Ahn, Shell Xu Hu, Andreas Damianou, Neil D Lawrence, and Zhenwen Dai. 2019. Variational information distillation for knowledge transfer. In *CVPR*. 9163–9171.
- [2] Charles Blundell, Julien Cornebise, Koray Kavukcuoglu, and Daan Wierstra. 2015. Weight uncertainty in neural network. In *ICML*. PMLR, 1613–1622.
- [3] Zhaowei Cai and Nuno Vasconcelos. 2018. Cascade r-cnn: Delving into high quality object detection. In *CVPR*. 6154–6162.
- [4] Yevgen Chebotar and Austin Waters. 2016. Distilling knowledge from ensembles of neural networks for speech recognition. In *Interspeech*. 3439–3443.
- [5] Guobin Chen, Wongun Choi, Xiang Yu, Tony Han, and Manmohan Chandraker. 2017. Learning efficient object detection models with knowledge distillation. *NeurIPS* 30 (2017).
- [6] Kai Chen, Jiaqi Wang, Jiangmiao Pang, Yuhang Cao, Yu Xiong, Xiaoxiao Li, Shuyang Sun, Wansen Feng, Ziwei Liu, Jiarui Xu, et al. 2019. MMDetection: Open mmlab detection toolbox and benchmark. *arXiv preprint arXiv:1906.07155* (2019).
- [7] Liang-Chieh Chen, Yukun Zhu, George Papandreou, Florian Schroff, and Hartwig Adam. 2018. Encoder-decoder with atrous separable convolution for semantic image segmentation. In *ECCV*. 801–818.
- [8] MMSegmentation Contributors. 2020. MMSegmentation: OpenMMLab Semantic Segmentation Toolbox and Benchmark. <https://github.com/open-mmlab/mms Segmentation>.
- [9] MMRazor Contributors. 2021. OpenMMLab Model Compression Toolbox and Benchmark. <https://github.com/open-mmlab/mmrazor>.
- [10] MMPPreTrain Contributors. 2023. OpenMMLab's Pre-training Toolbox and Benchmark. <https://github.com/open-mmlab/mmpretrain>.
- [11] Marius Cordts, Mohamed Omran, Sebastian Ramos, Timo Rehfeld, Markus Enzweiler, Rodrigo Benenson, Uwe Franke, Stefan Roth, and Bernt Schiele. 2016. The Cityscapes Dataset for Semantic Urban Scene Understanding. In *CVPR*.
- [12] Xing Dai, Zeren Jiang, Zhao Wu, Yiping Bao, Zhicheng Wang, Si Liu, and Erjin Zhou. 2021. General instance distillation for object detection. In *CVPR*. 7842–7851.
- [13] Jia Deng, Wei Dong, Richard Socher, Li-Jia Li, Kai Li, and Li Fei-Fei. 2009. ImageNet: A large-scale hierarchical image database. In *CVPR*. 248–255. <https://doi.org/10.1109/CVPR.2009.5206848>
- [14] Shangchen Du, Shan You, Xiaojie Li, Jianlong Wu, Fei Wang, Chen Qian, and Changshui Zhang. 2020. Agree to disagree: Adaptive ensemble knowledge distillation in gradient space. *NeurIPS* 33 (2020), 12345–12355.
- [15] Zhixing Du, Rui Zhang, Ming-Fang Chang, Xishan Zhang, Shaoli Liu, Tianshi Chen, and Yunji Chen. 2021. Distilling Object Detectors with Feature Richness. In *NeurIPS*.
- [16] Takashi Fukuda, Masayuki Suzuki, Gakuto Kurata, Samuel Thomas, Jia Cui, and Bhuvana Ramabhadran. 2017. Efficient Knowledge Distillation from an Ensemble of Teachers. In *Interspeech*. 3697–3701.
- [17] Kaiming He, Xiangyu Zhang, Shaoqing Ren, and Jian Sun. 2016. Deep residual learning for image recognition. In *CVPR*. 770–778.
- [18] Geoffrey Hinton, Oriol Vinyals, and Jeff Dean. 2014. Distilling the knowledge in a neural network. *NeurIPS Workshop* (2014).
- [19] Jie Hu, Li Shen, and Gang Sun. 2018. Squeeze-and-excitation networks. In *CVPR*. 7132–7141.
- [20] Tao Huang, Yuan Zhang, Shan You, Fei Wang, Chen Qian, Jian Cao, and Chang Xu. 2022. Masked Distillation with Receptive Tokens. *arXiv preprint arXiv:2205.14589* (2022).
- [21] Alex Kendall and Yarin Gal. 2017. What uncertainties do we need in bayesian deep learning for computer vision? *NeurIPS* 30 (2017).
- [22] Durk P Kingma, Tim Salimans, and Max Welling. 2015. Variational dropout and the local reparameterization trick. *NeurIPS* 28 (2015).
- [23] Kisoo Kwon, Hwidong Na, Hoshik Lee, and Nam Soo Kim. 2020. Adaptive knowledge distillation based on entropy. In *ICASSP*. IEEE, 7409–7413.
- [24] Quanquan Li, Shengying Jin, and Junjie Yan. 2017. Mimicking very efficient network for object detection. In *CVPR*. 6356–6364.
- [25] Xiang Li, Wenhai Wang, Xiaolin Hu, and Jian Yang. 2019. Selective kernel networks. In *CVPR*. 510–519.
- [26] Tsung-Yi Lin, Piotr Dollár, Ross Girshick, Kaiming He, Bharath Hariharan, and Serge Belongie. 2017. Feature pyramid networks for object detection. In *CVPR*. 2117–2125.
- [27] Tsung-Yi Lin, Priya Goyal, Ross Girshick, Kaiming He, and Piotr Dollár. 2017. Focal loss for dense object detection. In *ICCV*. 2980–2988.
- [28] Tsung-Yi Lin, Michael Maire, Serge Belongie, James Hays, Pietro Perona, Deva Ramanan, Piotr Dollár, and C Lawrence Zitnick. 2014. Microsoft coco: Common objects in context. In *ECCV*. Springer, 740–755.
- [29] Yuang Liu, Wei Zhang, and Jun Wang. 2020. Adaptive multi-teacher multi-level knowledge distillation. *Neurocomputing* 415 (2020), 106–113.
- [30] Wonpyo Park, Dongju Kim, Yan Lu, and Minsu Cho. 2019. Relational knowledge distillation. In *CVPR*. 3967–3976.
- [31] Harish Guruprasad Ramaswamy et al. 2020. Ablation-cam: Visual explanations for deep convolutional network via gradient-free localization. In *WACV*. 983–991.
- [32] Shaoqing Ren, Kaiming He, Ross Girshick, and Jian Sun. 2015. Faster r-cnn: Towards real-time object detection with region proposal networks. *NeurIPS* 28 (2015).
- [33] Adriana Romero, Nicolas Ballas, Samira Ebrahimi Kahou, Antoine Chassang, Carlo Gatta, and Yoshua Bengio. 2015. Fitnets: Hints for thin deep nets. In *ICLR*.
- [34] Mark Sandler, Andrew Howard, Menglong Zhu, Andrey Zhmoginov, and Liang-Chieh Chen. 2018. Mobilenetv2: Inverted residuals and linear bottlenecks. In *CVPR*. 4510–4520.
- [35] Yichun Shi and Anil K Jain. 2019. Probabilistic face embeddings. In *ICCV*. 6902–6911.
- [36] Changyong Shu, Yifan Liu, Jianfei Gao, Zheng Yan, and Chunhua Shen. 2021. Channel-Wise Knowledge Distillation for Dense Prediction. In *ICCV*. 5311–5320.
- [37] Roman Solov'yev, Weimin Wang, and Tatiana Gabruseva. 2021. Weighted boxes fusion: Ensembling boxes from different object detection models. *Image and Vision Computing* (2021), 1–6.
- [38] Yonglong Tian, Dilip Krishnan, and Phillip Isola. 2019. Contrastive Representation Distillation. In *ICLR*.
- [39] Zhi Tian, Chunhua Shen, Hao Chen, and Tong He. 2019. Fcos: Fully convolutional one-stage object detection. In *ICCV*. 9627–9636.
- [40] Tao Wang, Li Yuan, Xiaopeng Zhang, and Jiashi Feng. 2019. Distilling object detectors with fine-grained feature imitation. In *CVPR*. 4933–4942.
- [41] Zhenyu Wang, Yali Li, Ye Guo, Lu Fang, and Shengjin Wang. 2021. Data-uncertainty guided multi-phase learning for semi-supervised object detection. In *CVPR*. 4568–4577.
- [42] Sanghyun Woo, Jongchan Park, Joon-Young Lee, and In So Kweon. 2018. Cbam: Convolutional block attention module. In *ECCV*. 3–19.
- [43] Meng-Chieh Wu, Ching-Te Chiu, and Kun-Hsuan Wu. 2019. Multi-teacher knowledge distillation for compressed video action recognition on deep neural networks. In *ICASSP*. IEEE, 2202–2206.
- [44] Saining Xie, Ross Girshick, Piotr Dollár, Zhuowen Tu, and Kaiming He. 2017. Aggregated residual transformations for deep neural networks. In *CVPR*. 1492–1500.
- [45] Zhendong Yang, Zhe Li, Xiaohu Jiang, Yuan Gong, Zehuan Yuan, Danpei Zhao, and Chun Yuan. 2022. Focal and global knowledge distillation for detectors. In *CVPR*. 4643–4652.
- [46] Zhendong Yang, Zhe Li, Mingqi Shao, Dachuan Shi, Zehuan Yuan, and Chun Yuan. 2022. Masked Generative Distillation. In *ECCV*, Vol. 13671. Springer, 53–69.
- [47] Ze Yang, Shaohui Liu, Han Hu, Liwei Wang, and Stephen Lin. 2019. Reppoints: Point set representation for object detection. In *ICCV*. 9657–9666.
- [48] Shan You, Chang Xu, Chao Xu, and Dacheng Tao. 2017. Learning from multiple teacher networks. In *SIGKDD*. 1285–1294.
- [49] Fei Yuan, Linjun Shou, Jian Pei, Wutao Lin, Ming Gong, Yan Fu, and Daxin Jiang. 2021. Reinforced multi-teacher selection for knowledge distillation. In *AAAI*, Vol. 35. 14284–14291.
- [50] Sergey Zagoruyko and Nikos Komodakis. 2016. Paying more attention to attention: Improving the performance of convolutional neural networks via attention transfer. In *ICLR*.
- [51] Hailin Zhang, Defang Chen, and Can Wang. 2022. Confidence-aware multi-teacher knowledge distillation. In *ICASSP*. IEEE, 4498–4502.
- [52] Linfeng Zhang and Kaisheng Ma. 2020. Improve object detection with feature-based knowledge distillation: Towards accurate and efficient detectors. In *ICLR*.
- [53] Youcai Zhang, Zhonghao Lan, Yuchen Dai, Fangao Zeng, Yan Bai, Jie Chang, and Yichen Wei. 2020. Prime-aware adaptive distillation. In *ECCV*. Springer, 658–674.
- [54] Yuhang Zhang, Chengrui Wang, and Weihong Deng. 2021. Relative Uncertainty Learning for Facial Expression Recognition. *NeurIPS* 34 (2021), 17616–17627.
- [55] Hengshuang Zhao, Jianping Shi, Xiaojuan Qi, Xiaogang Wang, and Jiaya Jia. 2017. Pyramid scene parsing network. In *CVPR*. 2881–2890.
- [56] Kecheng Zheng, Cuiling Lan, Wenjun Zeng, Zhizheng Zhang, and Zheng-Jun Zha. 2021. Exploiting sample uncertainty for domain adaptive person re-identification. In *AAAI*, Vol. 35. 3538–3546.
- [57] Zhedong Zheng and Yi Yang. 2021. Rectifying pseudo label learning via uncertainty estimation for domain adaptive semantic segmentation. *IJCV* 129, 4 (2021), 1106–1120.
- [58] Xizhou Zhu, Dazhi Cheng, Zheng Zhang, Stephen Lin, and Jifeng Dai. 2019. An empirical study of spatial attention mechanisms in deep networks. In *ICCV*. 6688–6697.

Received 24 April 2023